Evidence for pheomelanin sheet structure

A D Davy[1] and D J S Birch[1, a)]
Photophysics Group, Department of Physics, SUPA, University of Strathclyde, Glasgow, G4 0NG, Scotland

(Dated: 22 November 2018)

Melanin remains one of the most enigmatic of pigments. It occurs in a variety of forms, but is perhaps best known for its role in providing ultra-violet protection of skin as brown/black eumelanin and red/yellow pheomelanin. Despite decades of research many questions remain about the structure, spectroscopy and biology of both forms. For example, their unusually broad optical absorption spectra have attracted different explanations, no protomolecule has ever been identified and pheomelanin has been implicated in melanoma, the most virulent form of skin cancer. Knowing more about the structure and spectroscopy of melanin is of paramount importance, not only in biology and medicine, but also in the design of biomimetic functional devices. There is general consistency across a variety of techniques that eumelanin's building blocks arrange in π-stacked sheets analogous to graphite. By comparison pheomelanin has been the neglected sibling and here we present evidence from fluorescence spectroscopy for pheomelanin also displaying sheet-like behavior. As pheomelanin is synthesized the temporal response of the fluorescence intensity of the sheet-sensing probe thioflavin T (ThT) follows a similar sigmoidal increase as previously reported for eumelanin. Consistent with such intercalation fluorescence decay measurements reveal evidence for close coupling between melanin and ThT excited states.

Keywords: Pheomelanin, eumelanin, thioflavin T, fluorescence, melanoma

Melanin is an important pigment found in human skin, hair, the eye and the brain and other organisms. In skin it occurs predominantly as the black/brown pigment eumelanin and also less frequently in the form of red/yellow pheomelanin. In vertebrates a complex melanogenesis pathway occurs in organelles called melanosomes within melanocytes[1] and requires the copper-containing enzyme tyrosinase to catalyze the oxidation of tyrosine and 3,4-dihydroxy-L-phenylalanine (L-DOPA) to form dopaquinone, which rapidly undergoes internal cyclization to form dopachrome and subsequently 5,6-dihydroxyindole (DHI) and 5,6-dihydroxyindole-2-carboxylic acid (DHICA) and their oxidized forms, which together constitute eumelanin. Pheomelanin follows a similar synthetic pathway up to dopaquinone, but then requires the addition of cysteine to form the precursor cysteinldopa leading to mainly sulfur-containing benzothiazine and benzothiazole derivatives[1] rather than DHI and DHICA. For both forms of melanin their broad-band absorption spectra from the ultra-violet to the near infra-red (Figure 1(a)) is generally taken to imply they are composed of a heterogenic polymeric mixture of different oligomers, each with their own spectroscopy, rather than replication of a protomolecule.

Eumelanin is thought to provide most of the ultra-violet protection in humans, carrying with it free radical scavenging properties of benefit in minimizing the susceptibility to skin cancer, the most virulent of which being melanoma. By contrast pheomelanin predominates in people with reddish hair and is thought to be implicated in producing cancer-inducing phototoxic species such as reactive oxygen species[2] and mutations.[3] The ratio of pheo- to eu-melanin has been demonstrated to be a potential cancer biomarker using two-photon excited fluorescence,[4–6] but the complexity of the approach makes it impractical and despite considerable research, optical biopsies have yet to replace excision in testing for melanoma. Nevertheless the urgent need for more practical and simpler alternatives to excision remains and optical approaches remain at the forefront of this area. The importance of such cancer biomarkers spans clinical progression as it is also of relevance in improving tumor margin estimation in optically-guided surgery.[7]

The coexistence of pheo- and eu-melanin and its relevance to optical biopsy for routine screening and cancer surgery are predicated on the need for improved spectroscopic descriptions and a better understanding of melanin's different structural forms. Moreover, the interest in melanin is not limited to biology and medicine as it is spurring on new ideas in biomimetics[8,9] due to melanin's unique combination of physical properties.[10] Here also the lack of knowledge about melanin's structure-spectroscopic relationship is an impediment to progress. Even melanin's much-studied broad absorption spectrum, which underpins its sun-screening properties, continues to attract different explanations. Early descriptions[10] included that of a semiconductor, distinct states and scattering, and more recently excitonic coupling[11] along with long-range water-induced coulombic interaction.[12] Melanin's intrinsic fluorescence has so far been similarly unrevealing as it is weak and complicated by overlapping bands,[13,14] thus offering little structural insight (Figure 1(b)).

Despite the conundrum melanin presents eumelanin's photophysical properties are thought to be determined

a)Author to whom correspondence should be addressed. Electronic mail: djs.birch@strath.ac.uk

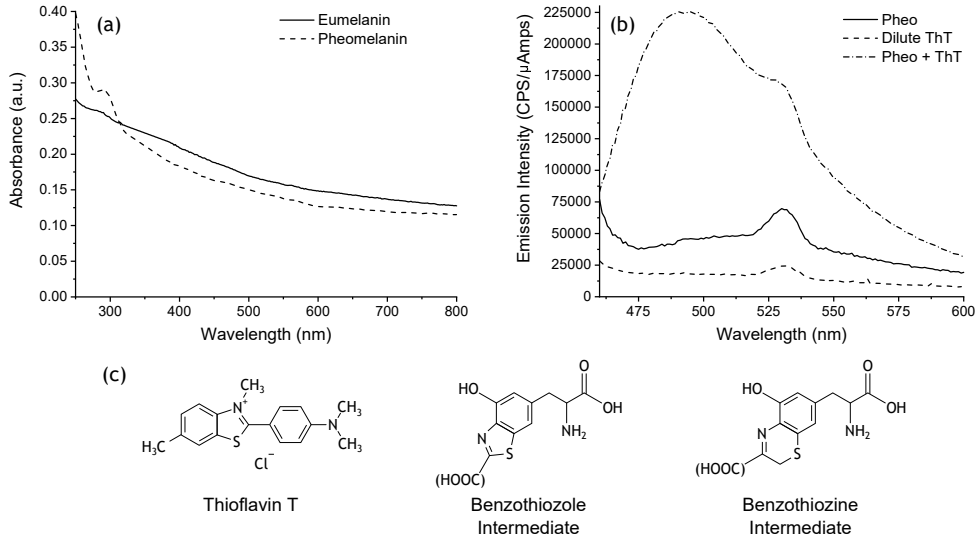

FIG. 1. (a) Absorption spectra of eumelanin and pheomelanin at 24 hours into the synthesis. (b) The fluorescence emission spectra of ThT (40 μM), pheomelanin (40 μM) and ThT in pheomelanin when excited at 450 nm, both pheomelanin measurements at 2 hours into the synthesis. The concentration of tyrosinase used was 750 u/ml. (c) The structures of ThT and pheomelanin's primary benzothiazole and benzothiazine groups are shown underneath.

by redox states of DHI and DHICA arranged in a sheet structure akin to graphite and bound by π-π^* interactions ($\sim$ 0.3 – 0.4 nm apart).[15,16] The evidence for this has been found from a number of sources including scanning electron microscopy (SEM) and atomic force microscopy (AFM).[17,18] Most importantly the manner in which pheomelanin's moieties are arranged is much less well-established than for eumelanin. Perhaps somewhat surprisingly there are few reports of the use of extrinsic fluorescence probes to study melanin structure. Previously our Group obtained complementary evidence of a sheet structure in eumelanin[19] to that from SEM and AFM by monitoring the laboratory synthesis of eumelanin using the fluorescence intensity of thioflavin T (ThT), which is commonly used to monitor formation of β-sheets of β–amyloid (Aβ) which lead to fibril formation associated with Alzheimer's disease.[20] Here we apply the same approach to the synthesis of pheomelanin and extended it to fluorescence decay measurements for both forms in order that we can provide a more comprehensive comparison with the work reported previously, which was limited to fluorescence spectral and intensity information.[19] In contrast to the indole structure of eumelanin's building blocks both ThT and pheomelanin's building blocks share some structural similarities (Figure 1(c)), which on the face of it should benefit the intercalation and improve ThT's sheet sensing capability. However, previously it was suggested that pheomelanin would be less likely than eumelanin to form flat sheets due to steric hindrance,[21]. In addition there are fewer cross-linking binding sites in pheomelanin's building blocks than there are in eumelanin[1] and this may also limit sheet formation in pheomelanin. Nevertheless our findings are consistent with sheet formation. Indeed the use of fluorescence lifetime distribution analysis rather than discrete component analysis may well shed light on the relative degree of heterogeneity of both forms, but, as we show later, the relative amplitude of discrete decay components may also provide some useful information on this.

L-DOPA, >98%, L-Cysteine, >97%, tyrosinase from mushroom with 2687 enzymatic units per mg (u/mg) and ThT were used as supplied by Sigma-Aldrich. Stock solutions of each reactant were made by mixing each compound with distilled water such that the final concentration became 3 mM for L-DOPA and cysteine, 1 mM for ThT and 1500 u/ml for tyrosinase. The stock solution of L-DOPA was sonicated for 5-10 mins to ensure the powder had completely dissolved. The pH of the samples was within the range of 6.4 and 7.0. Mixing the solutions for measurement followed previous studies where a concentration of 40 μM L-DOPA and 40 μM ThT was used.[19] Specifically, 125 μl of ThT was added to 3 ml of distilled water, followed by 125 μl of melanin solution. The pheomelanin synthesis followed the protocol of D'Ischia et al[22] where concentrations of L-DOPA and cysteine had a ratio of 1 mM:1 mM and the tyrosinase concentration were diluted to 500 enzymatic units per ml (u/ml) and 750 u/ml. For eumelanin samples, 40 μM of L-DOPA and 40 μM ThT were mixed in distilled water with a solution of ammonium hydroxide prepared via dilution of ammonium hydroxide (max 33% NH_3) solution (Sigma Aldrich) with distilled water. A HORIBA pH meter (model D-51) was used to monitor the pH of 50 ml of distilled water as the ammonium hydroxide solution was added. The volume of ammonium hydroxide needed to increase the pH to 10 was 10 μl. Prior to measurement, the diluted samples were aspirated 3 times with a 1 ml

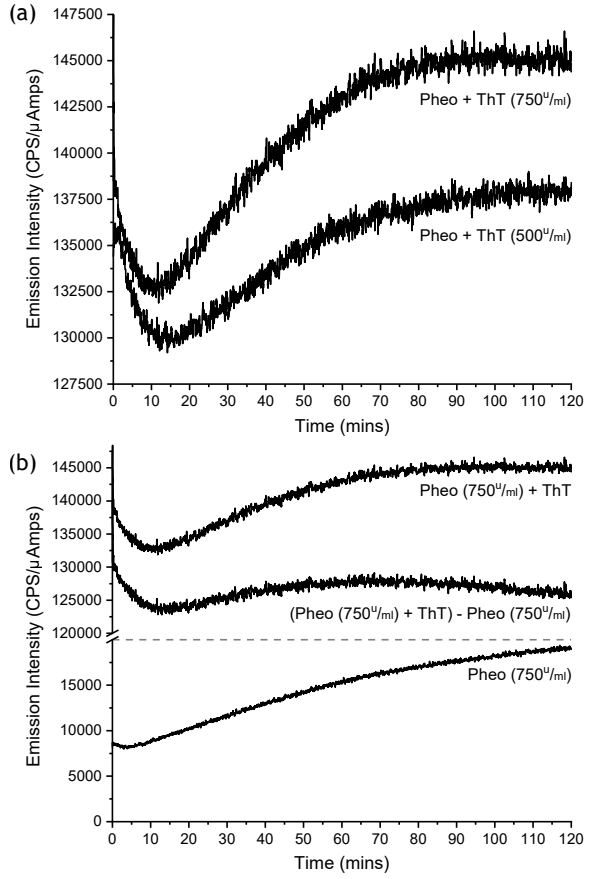

FIG. 2. (a) Change in fluorescence at 490 nm excited at 450 nm during pheomelanin synthesis with the addition of ThT at 750u/ml and 500u/ml concentrations of tyrosinase. (b) Rescaled pheomelanin + ThT at 750 u/ml tyrosinase curve from (a), intrinsic fluorescence of pheomelanin under the same conditions and the effect of subtracting the intrinsic fluorescence. The latter curve as illustrated was subtracted, the anomalous decrease in fluorescence after $\sim$ 70 mins suggesting ThT and pheomelanin are coupled rather than photophysically isolated.

pipette to ensure adequate mixing of reactants and then sealed with Parafilm®.

All spectral measurements were performed in 4 ml, clear wall, UV grade, plastic cuvettes (Fisher Scientific). Absorption measurements were obtained using a Perkin-Elmer Lambda 25 spectrophotometer. The wavelength range was 250 nm to 1100 nm with a scan speed of 960 nm/min. Empty cuvettes filled with distilled water were used in a reference channel to correct for solvent absorption. Fluorescence spectra were measured using a HORIBA Scientific FluoroMax 2 fluorimeter. Time series data were obtained with the excitation monochromator set to 450 nm and the emission monochromator set to 490 nm. The integration time and the measurement time interval was 1 second. Optical bandwidths were fixed at 4 nm for both excitation and emission. The total number of data points was 7200, which equated to a 2 hour measurement window. A 7x2 mm stir bar was set to keep the solution mixed but avoid vortex formation.

Fluorescence lifetime measurement and reconvolution analysis were performed on a DeltaFlex with DAS6 software (HORIBA Jobin Yvon IBH, Glasgow). For excitation, a NanoLED laser diode at 437 nm with a 1 MHz repetition rate and $<$ 200 ps pulse width, was used.[23] The emission monochromator was set to 490 nm at a bandwidth of 32 nm. A 450 nm long pass filter in the emission path reduced Rayleigh scatter. The emission polarizer was set to the magic angle (55°) with respect to the excitation polarizer to eliminate polarization effects. Scattering from dilute LUDOX® was used to record the instrumental response function. Measurements were concluded when the peak count reached 10,000.

ThT is a molecular rotor probe as its benzothiazole and aminobenzene rings form a twisted intramolecular charge transfer (TICT) state with a negligible fluorescence quantum yield in low viscosity solvents (Figure 1(b)), the yield increasing at higher viscosities.[24] When pheomelanin is formed in the presence of ThT and excited at 450 nm a spectral peak emerges at 490 nm which mirrors previous studies of ThT and eumelanin.[19] (The peak at $\sim$ 530 nm being consistent with the water Raman peak). Hence we chose 450 nm as an excitation wavelength and 490 nm as the fluorescence wavelength in order to best monitor ThT fluorescence rather than pheomelanin fluorescence. Figure 2(a) charts this growth in fluorescence and Figures 2(b) and 1(b) together show that ThT dominates the fluorescence when added to pheomelanin, the latter having a quantum yield as low as 10^{-4} depending on excitation wavelength.[25] Interestingly, an initial drop in fluorescence is evident in Figure 2(a). (Note there is also a much smaller initial decrease in pheomelanin intrinsic fluorescence). A likely explanation of this is that in the early stages the precursor structures of pheomelanin transfer their energy to ThT, which has a lower fluorescence quantum yield until bound within sheets, thus effectively quenching their fluorescence. Eumelanin with ThT shows similar behavior. Initially some collisional quenching can occur but as the ThT loosely binds to the pheomelanin precursors static quenching would be likely to dominate due to ThT's TICT state. Subsequent increase in fluorescence suggests that ThT intramolecular rotation eventually becomes constrained within sheets. This conclusion holds even if ThT becomes polymerized within pheomelanin as in this case its fluorescence would be expected to be quenched just as pheomelanin's intrinsic fluorescence is.

Ignoring any pheomelanin-ThT interaction, and subtracting the pheomelanin intrinsic fluorescence in the manner previously used for eumlanin,[19] the apparent increase in ThT fluorescence as pheomelanin is formed is considerably less than that for eumelanin (Figure 2(b)), implying on the face of it less evidence for ThT intercalation in a sheet structure. The fall in fluorescence after $\sim$ 70 mins might in itself suggest that any sheet structure is unraveling but that seems unlikely. This brings into ques-

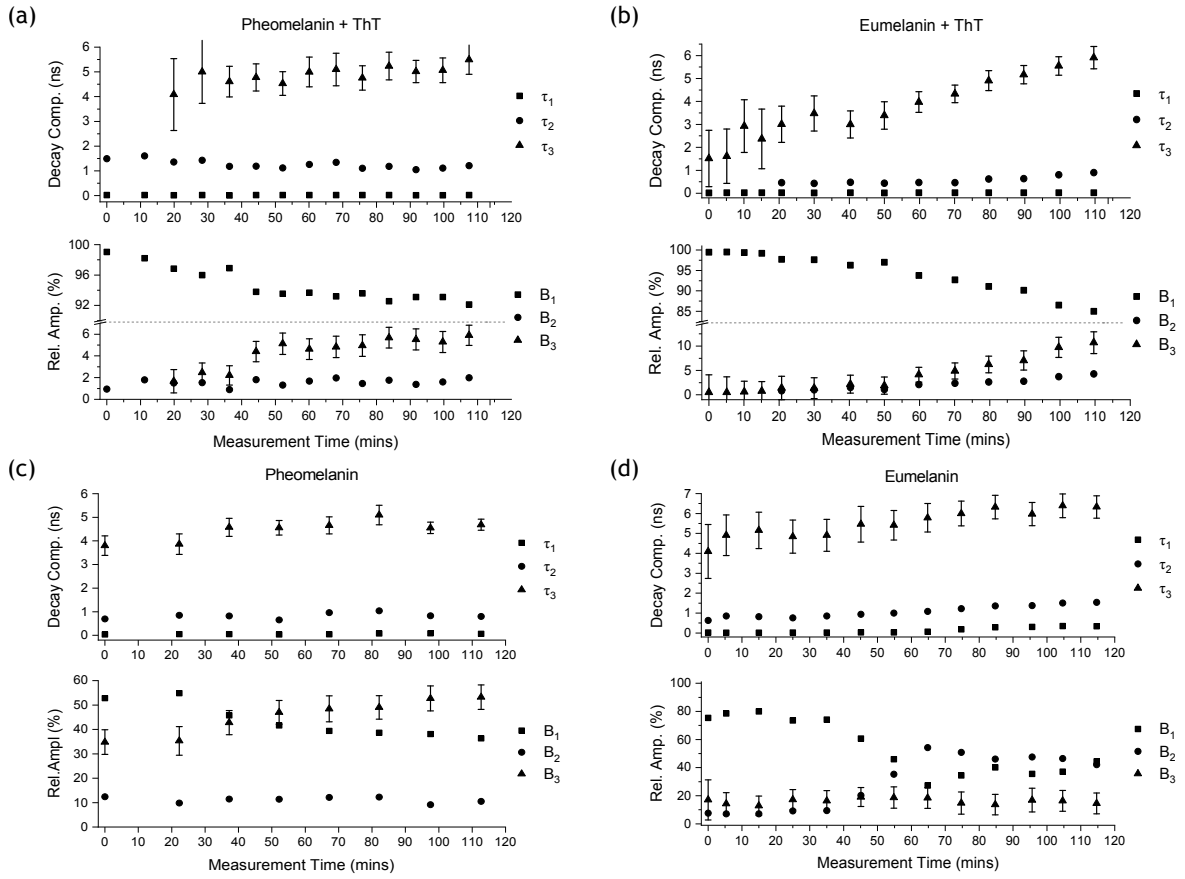

FIG. 3. Fluorescence decay fitted parameters as a function of synthesis time for (a) ThT and pheomelanin, (b) ThT and eumelanin, (c) pheomelanin and (d) eumelanin. For both melanins with ThT the early stages were best described by a two-exponential model until sheet structures started to be formed and thenceforth the measured decays fitted best to a three-exponential model. The intrinsic pheomelanin and eumelanin decay fitted to three-exponentials from the outset. Error bars of 3 std. dev. are shown for the decay time τ_3 and its relative amplitude B_3.

tion the validity, in this case, of treating pheomelanin and ThT in isolation and subtracting the pheomelanin fluorescence, thus providing evidence for electronic coupling between ThT and pheomelanin rather than them acting as isolated entities. Following the initial transient decrease and up to 100 mins the original 750 u/ml fluorescence growth curve shown in Figure 2(a) and the corresponding curve with pheomelanin intrinsic fluorescence subtracted up to 70 mins, as shown in Figure 2(b), can both be described by a similar sigmoidal function to that for eumelanin[19] i.e.

$$I(t) \sim I(0) + \alpha/\{1 + exp[-k(t - t_0)]\} \qquad (1)$$

Where I(t) is the fluorescence intensity and I(0) is the initial or background fluorescence intensity level. The parameter α is the fluorescence maximum above the background, k is the rate of melanin formation and t_0 the time where the fluorescence intensity has reached the half maximum value. The fitted values are shown in Table I along with the reduced chi-squared (χ^2) and compared with that previously reported for ThT and eumelanin. There are similarities in the values found for both forms of melanin with the presence of the enzyme tyrosinase with pheomelanin reducing the time delay t_0 for sheets to be formed and the rate of sheet formation to half that of eumelanin. The effect of subtracting pheomelanin intrinsic fluorescence is included in Table I for comparison as it still displays evidence for sheet formation by fitting to Eq.1.

TABLE I. Values for pheomelanin and ThT obtained from fitting a sigmoidal function to the normalized fluorescence growth curves of Figure 2 compared to those published previously for ThT and eumelanin.[19]

Sample	I(0)	α	k (min^{-1})	t_0 (mins)	χ^2
Pheo + ThT (750 u/ml)	-0.20	1.128	0.061	31.1	0.99
(Pheo + ThT) - Pheo	-0.0023	0.83	0.092	28.8	0.93
Eumelanin + ThT[19]	-0.062	1.19	0.17	48.6	-

Looking for further insight into the interactions between melanin and ThT we measured fluorescence decay components of ThT in both pheomelanin and eumelanin (Figure 3(a) and (b)). Prior to $\sim$ 20 mins both forms

of melanin with ThT present offered no improvement in reduced χ^2 by fitting to more than 2-exponentials as the decay is dominated by free ThT in water ($\tau_1 \sim 20$ ps, relative amplitude $> 97\%$). Beyond 20 mins 3-exponentials consistently gave a better description for ThT in both forms ($\chi^2 \leq 1.2$ for ThT-pheomelanin). One component (τ_3), increasing in ThT-pheomelanin up to ~ 5 ns and in ThT-eumelanin up to ~ 6 ns, is associated with the fluorescence increase. Previous work has shown that for ThT in Aβ and protein sheets the longest decay component is ~ 2 ns[26,27] and the pure radiative decay time in glycerol to be 3.4 ns.[24] Hence the ThT decay component we observe to increase up to ~ 5 ns in pheomelanin and ~ 6 ns in eumelanin correlates with ~ 5 ns component for pheomelanin intrinsic fluorescence and ~ 6 ns for eumelanin intrinsic fluorescence shown in Figures 3(c) and 3(d) respectively. This implies coupling between the excited states of melanin and ThT bound in sheets. The detailed nature of this interaction, and indeed energy transfer mechanisms, warrants further investigation beyond the scope of this present work, though Dexter exchange interaction, resonance energy transfer and exciton diffusion are all possible. The slightly higher average ThT-pheomelanin value for $\langle\tau_3\rangle$ (4.96 ns), in comparison to that for pheomelanin without ThT (4.72 ns), also bears testimony to close coupling modifying the radiative rates when ThT is intercalated within sheets. Moreover, the constancy in decay components and relative abundance of τ_2 after ~ 70 mins in both Figures 3(a) in the presence of ThT, and Figure 3(c) without ThT, and the relative increase in average τ_2 value with ThT ($\langle\tau_2\rangle =$ 0.86 to 1.26 ns), suggests that ThT also dominates this component. Given the likely distribution of ThT locations within pheomelanin τ_2 may well originate from sites with less sheet structure. The increase in relative abundance B_3 of τ_3 for ThT in eumelanin ($\sim 12\%$) compared to ThT in pheomelanin ($\sim 6\%$) would be consistent with increased sheet formation in eumelanin and indeed could be a useful descriptor of the degree of heterogeneity.[21] For ThT in both pheomelanin and eumelanin τ_3 and B_3 provide unequivocal evidence that it is not just melanin intrinsic fluorescence which is being tracked. For example in Figure 3 B_3 for pheomelanin rises to $\sim 50\%$ but is only $\sim 6\%$ when ThT is added and in the case of eumelanin B_3 remains fairly constant at $\sim 17\%$ whereas in the presence of ThT gradually increases to $\sim 6\%$. Methods of describing and discriminating between pheomelanin and eumelanin are clearly important in medical applications[4–7] and the fluorescence decay of a probe such as ThT, which we describe here, potentially offers a simpler approach than ultrafast methods such as two-photon excitation[4–6] and transient absorption.[28]

It is important to keep in mind that because pheomelanin is complex, incorporating numerous heterogenic structures capable of excitation and emission, exponential decay component analysis should be viewed as an approximation. However, together the dominant fluorescence intensity of ThT with pheomelanin shown in Figures 1(b) and 2, and the trends in fluorescence decay parameters in Figure 3, support interpretation in terms of sheet formation.

See supplementary material for the fluorescence decay data and associated tables of fitted parameters.

The authors would like to thank the EPSRC and MRC OPTIMA CDT for the provision of a research studentship for ADD and NPL for financial support.

[1] S. Ito, Pigment Cell Res. **16**, 230 (2003).
[2] R. Micillo, L. Panzella, K. Koike, G. Monfrecola, A. Napolitano, and M. D'Ischia, Int. J. Mol. Sci. **17** (2016).
[3] T. H. Nasti and L. Timares, Photochem. Photobiol. **91**, 188 (2015).
[4] K. Teuchner, W. Freyer, D. Leupold, A. Volkmer, D. J. Birch, P. Altmeyer, M. Stücker, and K. Hoffmann, Photochem. Photobiol. **70**, 146 (1999).
[5] D. Leupold, M. Scholz, G. Stankovic, J. Reda, S. Buder, R. Eichhorn, G. Wessler, M. Stücker, K. Hoffmann, J. Bauer, and C. Garbe, Pigment Cell Melanoma Res. **24**, 438 (2011).
[6] T. B. Krasieva, C. Stringari, F. Liu, C.-H. Sun, Y. Kong, M. Balu, F. L. Meyskens, E. Gratton, and B. J. Tromberg, J. Biomed. Opt. **18**, 31107 (2013).
[7] A. V. DSouza, H. Lin, E. R. Henderson, K. S. Samkoe, and B. W. Pogue, J. Biomed. Opt. **21**, 080901 (2016).
[8] M. Ambrico, P. F. Ambrico, T. Ligonzo, A. Cardone, S. R. Cicco, A. Lavizzera, V. Augelli, and G. M. Farinola, Appl. Phys. Lett. **100**, 253702 (2012).
[9] T. Guin, J. H. Cho, F. Xiang, C. J. Ellison, and J. C. Grunlan, ACS Macro Lett. **4**, 335 (2015).
[10] P. Meredith and T. Sarna, Pigment Cell Res. **19**, 572 (2006).
[11] C. T. Chen, C. Chuang, J. Cao, V. Ball, D. Ruch, and M. J. Buehler, Nat. Commun. **5**, 1 (2014).
[12] L. B. Assis Oliveira, L. F. Tertius, B. J. Costa Cabral, K. Coutinho, and S. Canuto, J. Chem. Phys. **145** (2016).
[13] S. P. Nighswander-Rempel, J. Riesz, J. Gilmore, and P. Meredith, J. Chem. Phys. **123** (2005).
[14] P. Yip and J. U. Sutter, Methods Appl. Fluoresc. **6**, 027001 (2018).
[15] G. W. Zajac, J. M. Gallas, M. Eisner, and S. C. Moss, Biochim. Biophys. **1199**, 271 (1994).
[16] J. Cheng, S. C. Moss, and M. Eisner, Pigment Cell Melanoma Res. **7**, 263 (1994).
[17] Y. Liu and J. D. Simon, Pigment Cell Res. **16**, 72 (2003).
[18] C. M. R. Clancy and J. D. Simon, Biochemistry **40**, 13353 (2001).
[19] J. U. Sutter, T. Bidláková, J. Karolin, and D. J. S. Birch, Appl. Phys. Lett. **100**, 113701 (2012).
[20] N. Benseny-Cases, M. Cócera, and J. Cladera, Biochem. Biophys. Res. Commun. **361**, 916 (2007).
[21] J. Riesz, T. Sarna, and P. Meredith, J. Phys. Chem. B **110**, 13985 (2006).
[22] M. D'Ischia, K. Wakamatsu, A. Napolitano, S. Briganti, J. C. Garcia-Borron, D. Kovacs, P. Meredith, A. Pezzella, M. Picardo, T. Sarna, J. D. Simon, and S. Ito, Pigment Cell Melanoma Res. **26**, 616 (2013).
[23] C. D. McGuinness, K. Sagoo, D. McLoskey, and D. J. Birch, Meas. Sci. Technol. **15** (2004).
[24] V. I. Stsiapura, A. A. Maskevich, V. A. Kuzmitsky, V. N. Uversky, I. M. Kuznetsova, and K. K. Turoverov, J. Phys. Chem. B **112**, 15893 (2008).
[25] S. P. Nighswander-Rempel, Biopolymers **82**, 631 (2006).
[26] S. Freire, M. H. De Araujo, W. Al-Soufi, and M. Novo, Dye. Pigment. **110**, 97 (2014).
[27] J. Mohanty, S. Dutta Choudhury, H. Pal, and A. C. Bhasikuttan, Chem. Commun. **48**, 2403 (2012).
[28] T. Ye and J. D. Simon, The Journal of Physical Chemistry B **107**, 11240 (2003).